Jurnal Teknologi

Full Paper

NUMERICAL STUDY OF THE RESISTANCE REDUCTION IN HYBRID MINI-SUBMARINE

F. A. Rayhan*, T. A. Nugraha, H. R. Akhira, Y. Pratiwi, R. Hatuwe

Naval Architecture and Marine Engineering, Universitas Pembangunan Nasional Veteran Jakarta, Jakarta, Indonesia 12450

Article history
Received
31 July 2023
Received in revised form
3 March 2024
Accepted
28 April 2024
Published Online
23 June 2024

*Corresponding author
fajri.ar@upnvj.ac.id

Graphical abstract

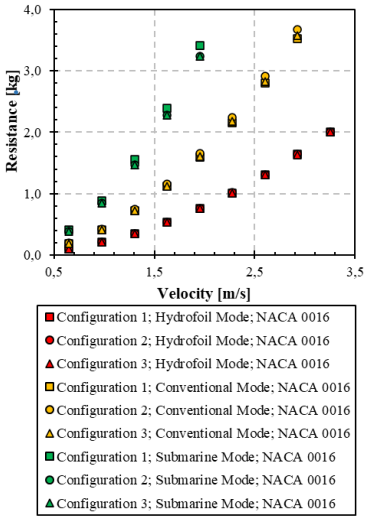

Abstract

Hybrid mini-submarine is a single innovative ship combining the concepts of conventional fast ships, hydrofoils, and submarine with the specific mission of safeguarding national sovereignty. This study was conducted to analyze the reduction of resistance in this mini-submarine by examining the positioning and shape of NACA hydrofoils. The process involved adjusting the positions of NACA hydrofoils and incorporating different configurations. This was indicated by the inclusion of nine speed configuration in the hydrofoil mode, eight in the conventional mode, and five in the submarine mode. Moreover, Computational Fluid Dynamics (CFD) simulation was applied for analysis using the Ansys CFX software. The results showed that the positioning of the NACA hydrofoils at close proximity reduced the resistance. The selection of symmetrical and slender configuration was also observed to optimize the reduction of resistance. Moreover, the combination of position and NACA hydrofoil 0012 produced an average resistance reduction of up to 12.52%. The configured model successfully reduced the total ship resistance and also identified the optimal position and shape configuration for the NACA hydrofoils. These findings provided valuable insights into the components and characteristics of total ship resistance and served as a valuable reference for further research on the development of maritime security technology.

Keywords: Hybrid mini-submarine, resistance, hydrofoil, NACA, CFD

1.0 INTRODUCTION

The expansive maritime borders of Indonesia are posing a substantial threat and challenge to the country, leading the government and society to confront a formidable task of preserving its marine resources. This urgency is associated with the fact that 95% of the country's marine ecosystem faces endangerment due to destructive fishing practices, illegal, unreported and unregulated (IUU) fishing, river basin-based pollution, and coastal development [1]. The threat of maritime crime in the country is expected to continue growing in line with the increasing economic activity in Indonesian waters. The most prevalent crimes include piracy, robbery, and illegal fishing. Meanwhile, maritime laws are identified to be poorly enforced in the coastal states and this is affecting the sovereignty, security, and safety of affected countries [2]. The threats identified led to the development of a hybrid mini-submarine capable of operating in three modes including the (i) conventional, (ii) hydrofoil, and (iii) submarine modes. This hybrid mini-submarine is designed to have high speed in order to ensure it has the ability to chase

maritime criminals. Meanwhile, the market demand for different types and dimensions of multihull ships designed for low resistance and high speed has made optimization process important for these ships [3]. A high-speed ship usually generates a significant resistance and this led to the introduction of an additional structure called a hydrofoil which is placed beneath the ship's body and can be adjusted to the mode being used.

The hydrofoil principles are similar to those in aerofoil in aircraft wings, except that they are usually installed beneath the hull of a ship. Hydrofoils generally work like aerofoils but exhibit certain fundamental differences related to the design and operation including the (i) changes in fluid density, Reynolds Number (Re), (ii) differences in flow characteristics, and (iii) the possibility of cavitation [4]. The hydrofoils installed beneath the hull of a ship can provide lift to the ship's body, causing it to rise above the surface of the water. This occurs because the weight of the ship is supported by the foil, thereby reducing the surface area of the hull submerged in water and minimizing drag caused by friction between the hull and water. Furthermore, this lift force is normally experienced when the speed of the ship is increased.

The findings of a previous study showed that the inclusion of National Advisory Committee for Aeronautics (NACA) 63(2)-615 hydrofoil in multihull ships reduced the resistance by up to 37.56% [5]. Another study on a fast patrol ship equipped with NACA 4412 stern foil structure showed a 26.70% optimal reduction in total resistance [6]. The application of hydrofoils on high-speed multihull ships was also analyzed under different operating conditions and EPPLER 385 hydrofoil was observed to have reduced the resistance by up to 50% at a speed of 50 knots [7]. Moreover, the effect of stratified fluid density on submarines was studied and the findings showed the significant influence of the forward speed on ship resistance. The wave-making resistance coefficient was observed to reach a maximum point near Fr = 0.5 due to the destructive interference of stratified and uniform fluid waves on the submarine [8]. Furthermore, the hydrodynamic performance of submarine was investigated numerically under resistance and wave testing using pressure resistance reduction techniques. The results showed that the drag force increased up to 150% in resistance and wave testing due to the influence of free surface water [9]. The drag coefficient at full submersion depth for numerical and experimental evaluations was also observed to be differed by up to 13.3%. Meanwhile, it was discovered that there are no previous studies on hybrid submarines.

A hybrid mini-submarine was studied by [10] and found to have the ability to operate in three conditions including the (i) diving, (ii) floating, and (iii) foil modes. The main purpose of this innovative design was to create a reliable hybrid ship in all conditions and research was conducted experimentally with the data obtained tested using the Agency for the Assessment and Application of Technology (BPPT) towing tank with a length of 60 m, width of 35 m, and a depth of 2.5 m. The three ship modes were tested at a speed range of 0.6507 m/s to 3.2534 m/s on a 1.1 m long model ship. Moreover, the configurations of NACA 0016 hydrofoil with an aft foil strut distance of 0.195 m placed behind the midship and the fore foil strut distance of 0.367 m located in front of the midship were compared. Another study also conducted a numerical and experimental study on a crocodile ship designed based on the philosophy that crocodiles can swim both on the surface or inside the water [11]. The experiment was conducted using towing tank while the numerical aspect was based on the Reynolds Averaged Navier Stokes Equation (RANS) and K-epsilon turbulent model. The results showed that the hydrofoil mode produced less resistance than the diving mode. However, it was discovered that no previous studies focused on the hybrid submarine designed to include changes in the types and positions of the foils.

This study was conducted to analyze the resistance and fluid flow patterns associated with the changes in the position and shape of the hydrofoils on the hybrid mini-submarine. The process involved showing the smallest resistance linked to the variations in the position and shape of these hydrofoils using the Computational Fluid Dynamics (CFD) approach.

2.0 FUNDAMENTAL THEORY

The concept of total ship resistance was introduced in 1867 by William Froude consisting of two components including the residual and frictional resistance. The residual aspect encompasses the energy losses from wave-making systems, eddies, and viscous effects due to the shape of the ship's hull. Meanwhile, the frictional aspect is assumed to be equivalent to the frictional resistance of a two-dimensional flat plate with the same wetted surface area, moving through the water at the same speed as the ship.

The resistance of a ship is usually influenced by the ship's speed (V_s), the amount of water displaced by the submerged hull (Δ), and the shape of the hull [12]. The notation commonly used for ship total resistance is RT and it can be calculated using the following equation:

$$\mathrm{RT} = \frac{1}{2} \cdot \mathrm{C_T} \cdot \rho s \cdot \mathrm{V_S}^2 \quad (1)$$

Where, RT is the total resistance [N], $\mathrm{C_T}$ is the coefficient of total ship resistance [-], ρ is the fluid density [kg/m^3], s is the wetted surface area of the ship [m^2], and $\mathrm{V_S}$ is the ship speed [m/s].

The coefficient of frictional resistance was calculated using a regression equation based on the

Reynolds Number. The equation is expressed as follows:

$$C_F = \frac{0{,}075}{(\log_{Re} - 2)^2} \quad (2)$$

Where, C_F is the coefficient of frictional resistance [-] and the Re is the Reynolds Number [-] which can be calculated using the following equation:

$$Re = \frac{V_S \cdot L}{\vartheta} \quad (3)$$

Where, Re is the Reynolds Number [-], V_S is the ship speed [m/s], L is the length of the ship [m], and ϑ is the kinematic viscosity [m^2/s].

The wave resistance coefficient can be associated with the pressure differences generated by waves when a ship moves through a fluid. Therefore, the coefficient was calculated using the following equation:

$$C_W = C_T - C_V \quad (4)$$

Where, C_W is the wave resistance coefficient [-], C_T is the coefficient of total resistance [-], and C_V is the viscosity resistance coefficient [-].

The viscosity resistance coefficient is normally affected by the pressure variations on the hull due to the influence of the viscous flow. This coefficient can be calculated by multiplying the form factor by the friction coefficient as shown in the following equation:

$$C_V = (1 + k) \cdot C_F \quad (5)$$

Where, C_V is the viscosity resistance coefficient [-], C_F is the frictional resistance coefficient [-], and k is the form factor [-].

The additional resistance coefficient can be associated with the resistance experienced due to the activities of protruding devices on the ship's hull such as the shape of the stern, winglets, zinc anodes, rudders, and others. The value of the additional resistance can reach up to 10% of the total resistance and was determined using the following equation:

$$C_{APP} = \frac{R_{APP}}{\frac{1}{2}\rho \cdot s \cdot {V_S}^2} \quad (6)$$

Where, C_{APP} is the additional resistance coefficient [-] and R_{APP} is the additional resistance [N] calculated using the following equation:

$$R_{APP} = \frac{1}{2} \cdot \rho \cdot V_S \cdot s \cdot (1 + K_2) \cdot C_T \quad (7)$$

Where, $(1 + K_2)$ is the form factor [-] with a value of 2.8.

The governing equations for the solver include the Navier-Stokes in Equation 8 and the Continuity in Equation 9. These are further expressed in the following vector form:

$$\rho\left(\frac{\partial v}{\partial t} + V_S \cdot \nabla V_S\right) = -\nabla p + \mu \nabla^2 V_S + \rho g \quad (8)$$

$$\nabla \cdot V_S = 0 \quad (9)$$

Where, p is pressure [N/m^2], μ is dynamic viscosity [N·s/m^2], g represents gravitational acceleration [m/s^2], and ∇^2 is the Laplace Operator [-].

3.0 METHODOLOGY

The ship hull model is designed based on a 1:10.9 scale of the original ship's dimensions as indicated in Figure 1. Moreover, the foil struts were used to support the foils in their respective positions. The summary of the dimensions of the hybrid mini submarine is presented in the following Table 1.

The water draft utilized in the hydrofoil mode was 1.41 m as measured from the baseline and 0.08m for the conventional mode. According to [13], the water draft at standard depth for submarines under fully submerged conditions can be determined using the following relationship:

$$h = L/2 \quad (10)$$

Where, h represents the water draft from the water surface to the ship's baseline [m] and L denotes the overall length of the ship [m].

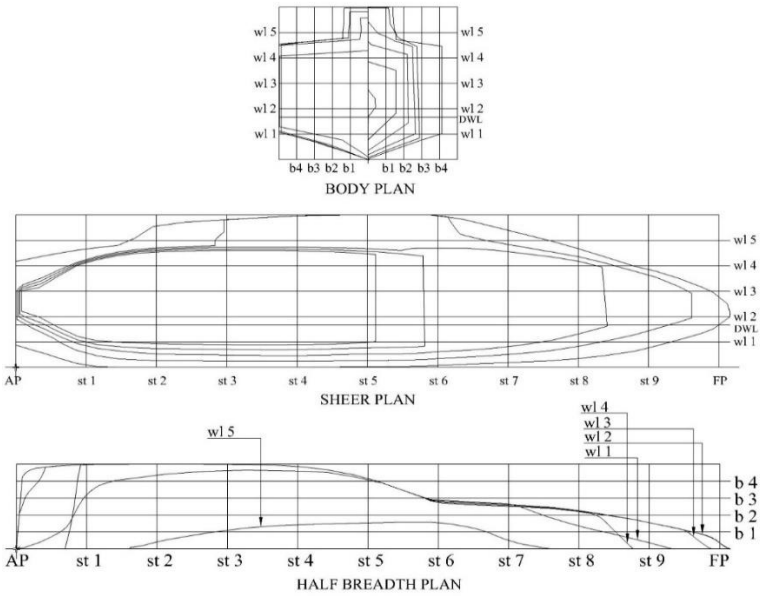

Figure 1 Lines plan of hybrid mini-submarine

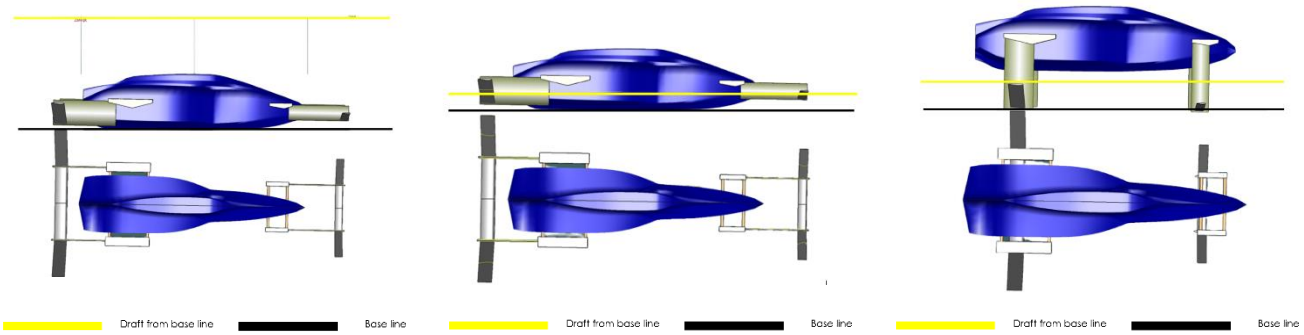

Figure 2 Ship mode: (a) Submarine, (b) conventional, and (c) hydrofoil

This means the water draft used for the submarine mode of hybrid mini-submarine was 0.55 m, calculated from the hydrofoil baseline.

The boundary conditions defined as the limiting surfaces created for the CFD simulations were established according to the International Towing Tank Convention (ITTC) 1957 rules. The conditions were generated in this study using Ansys ICEM based on the following distances including the inlet and outlet boundaries extending 2 times the model's LPP, the side and bottom boundaries by the length of the LPP, and the top boundary extending by half the length as indicated in Figure 3.

Table 1 Hybrid mini submarine data

Types of Ship	Hybrid Mini-Submarine		
Model Dimensions	Length overall (LOA)	1.1	m
	Length Between Perpendiculars (LPP)	0.92	m
	Breadth (B)	0.28	m
	Depth (H)	0.28	m
Maximum Speed [10]	Submarine Mode	15	knot
	Conventional Mode	25	knot
	Hydrofoil Mode	35	knot
Draft Model from Base Line	Submarine Mode	0.55	m
	Conventional Mode	0.08	m
	Hydrofoil Mode	1.41	m
Fluid Properties	Types of Fluid	Sea Water	-
	Density	1025	kg/m^3

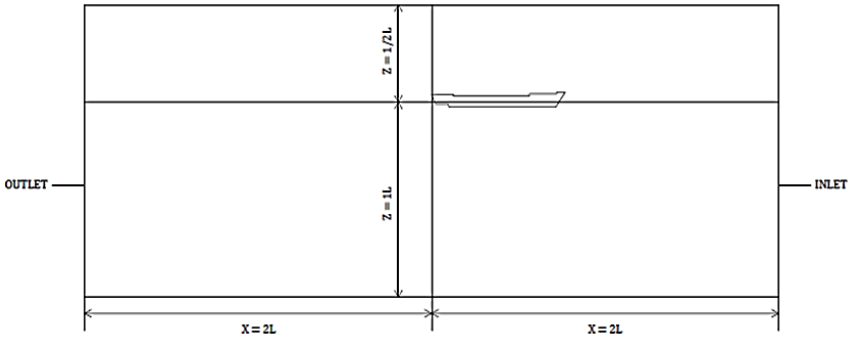

Figure 3 Boundary condition

The meshing quantity was determined by using a variation of 0.05 for the boundary and 0.0005 for the hull. This configuration was applied to achieve a dense meshing and ensure a high level of accuracy in the process.

Ansys CFX was set up to classify the boundary conditions created in the ICEM and this was applied to all the positions and ship modes. The process involved several steps and the first was the (i) domain boundary conditions which required the creation of two fluid domains including the water and air. The water domain had a temperature of 15°C while the air domain was assumed to be 25°C, reflecting the situation of the room, and an estimated ambient pressure of 1 atm. The domains were analyzed using the shear stress transport model previously validated as the most accurate for flow simulations [14]. The second was the (ii) inflow boundary conditions used to represent the direction of fluid flow coming from the front of the model. It was assumed that the model was stationary while the fluid flowed pass, thereby serving as the simulation of the same resistance conditions as when the ship was in operation. The fluid velocity for the water and air was specified while the air velocity was set at 0 to ensure there was no wind interference in the water conditions. The third was the (iii) outflow boundary conditions used to represent the direction of flow towards the rear. Average static pressure was used in this domain section based on the assumption that pressure was not generated by the waves produced in the model. The fourth was the (iv) bottom and side boundary conditions which were defined by the domain walls during the simulation process. The mass and momentum were set as free-slip walls to ensure the fluid velocity did not experience friction due to the presence of the walls. The fifth was the (v) model boundary conditions which had a wall and the mass and momentum set as no-slip walls in order to allow the fluid velocity to experience deceleration due to the friction against the model. The sixth was the (vi) convergence criteria which were set at a velocity of 1.63 m/s, a total of 2,843,511 elements, and a force of 5.39 N as shown in Figure 4.

Validation is a crucial step to determine the degree of agreement between the current and previous models [10]. This was achieved in this study using the total resistance experienced in the hydrofoil mode as the validation variable. The velocities ranged from 1.63 m/s to 3.25 m/s, thereby allowing a comparison between the results and those reported in previous studies.

$$\mathrm{MD} = \frac{1}{\mathrm{N}}\sum_{1}^{\mathrm{N}}\left|(\mathrm{dpre} - \mathrm{dexp}).\frac{100}{\mathrm{dexp}}\right| \tag{11}$$

Where, MD is mean deviation [-], N is the number of data points [-], dpre is the predicted or simulated data [N], and dexp is the experimental data [N].

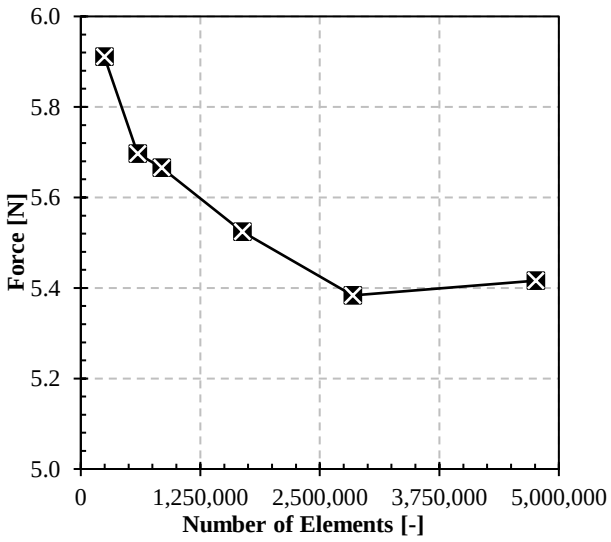

Figure 4 Convergence value

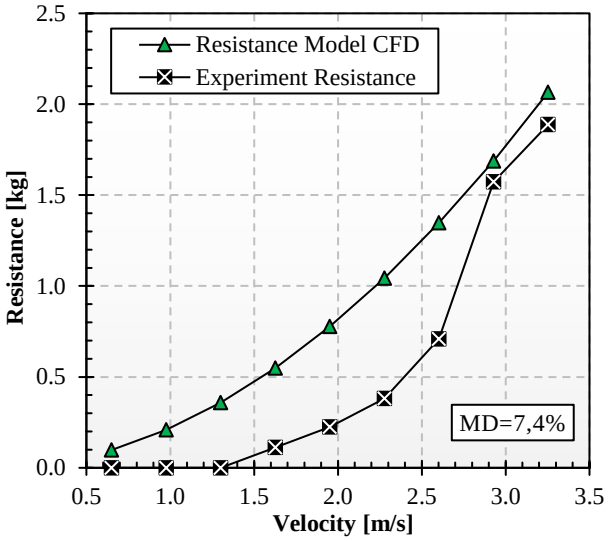

Figure 5 Validation of experiments and simulations

The determination of the validation data and graphs was followed by the calculation of the mean deviation, also known as the average deviation, and defined as the average distance between data values and their mean. The concept was used to identify the deviation of the data points from the mean and the results showed a difference of 7.4% between the simulated and experimental data, as shown in Figure 5. This means the data used in this research meet the required criteria.

The validation of the simulation data was followed by the presentation of the variations in the hydrofoil position configurations as indicated in Figure 6. This was conducted to determine the configuration with the minimum resistance. There are several abbreviations in Figure 5, including: AP (After Peak), FP (Fore Peak), MS (Midship Section), and DWL (Draft Water Line). The detailed information on the variations in these configurations is presented in the following Table 2.

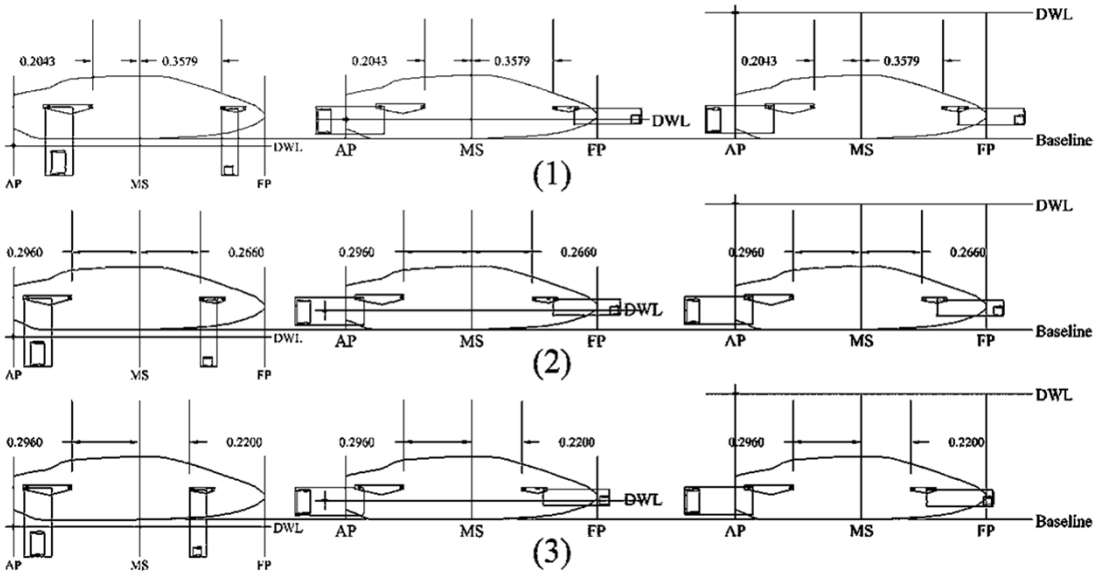

Figure 6 Variations in the configuration of the hybrid mini-submarine

Table 2 Testing conditions

Velocity Variation [m/s]	Hydrofoil Mode [m/s]	0.65 - 3.25	
	Conventional Mode [m/s]	0.65 - 2.93	
	Submarine Mode [m/s]	0.65 - 1,95	
Position Variation		***Aft Foil* [m]**	***Fore Foil* [m]**
	Configuration 1	-0.2043	+0.3579
	Configuration 2	-0.2960	+0.2660
	Configuration 3	-0.1375	+0.2200
Hydrofoil Variation	NACA 0016 and NACA 0012		

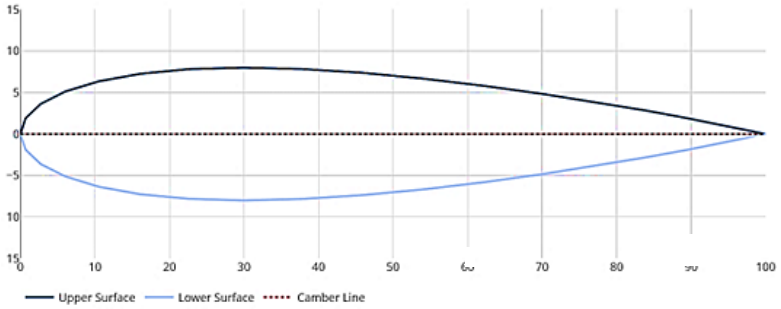

Figure 7 NACA 0016

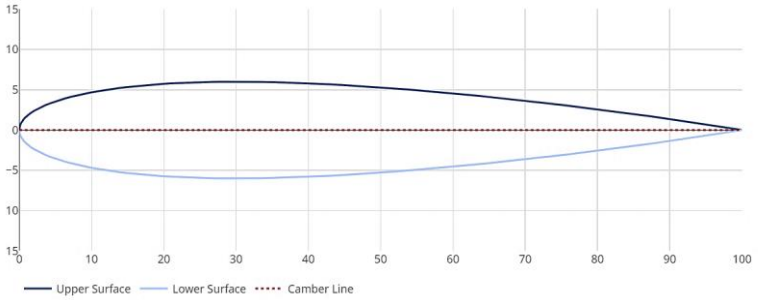

Figure 8 NACA 0012

4.0 RESULT AND DISCUSSION

The impact of configuration and velocity on ship resistance was presented in Figure 9 and the results showed that the ship resistance generally increased with the velocity. The hydrofoil mode was observed to have exhibited lower resistance values compared to the conventional and submarine modes. Moreover, the simulation results indicated that the NACA 0016 configuration in hydrofoil mode 3 produced the lowest total resistance of 48% compared to configuration 1 representing the submarine mode. This confirmed that the hydrofoil mode experienced the least resistance due to its smaller wetted surface area compared to the other modes. The result was further corroborated by [15] that the use of hydrofoil bubble generators reduced resistance by up to 25% in tested ships and this led to a significant enhancement of ship efficiency. Consequently, the incorporation of resistance-reducing hydrofoil technology was able to reduce the operational costs and mitigate the environmental impact of marine transportation.

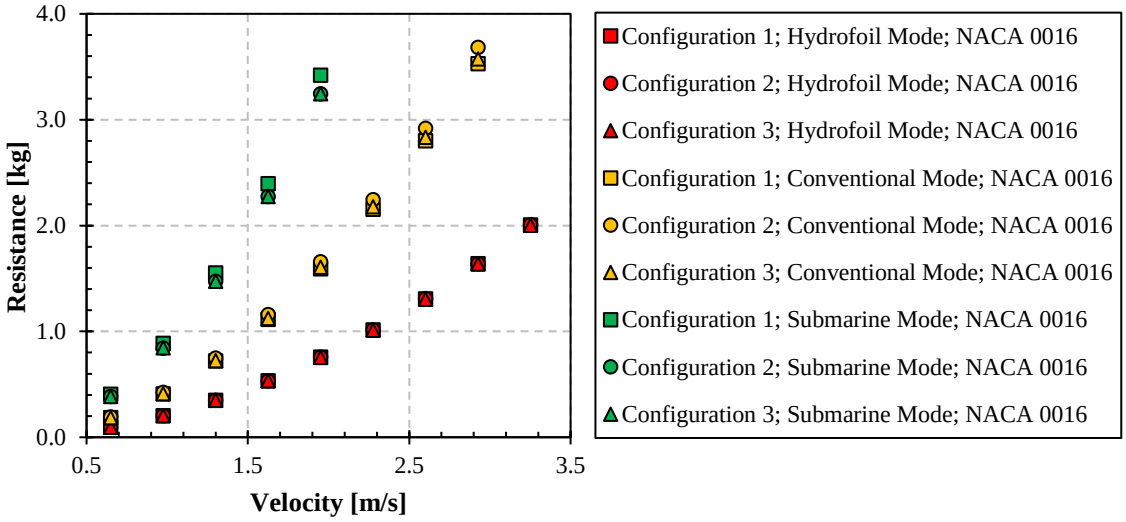

Figure 9 Ship resistance for NACA 0016

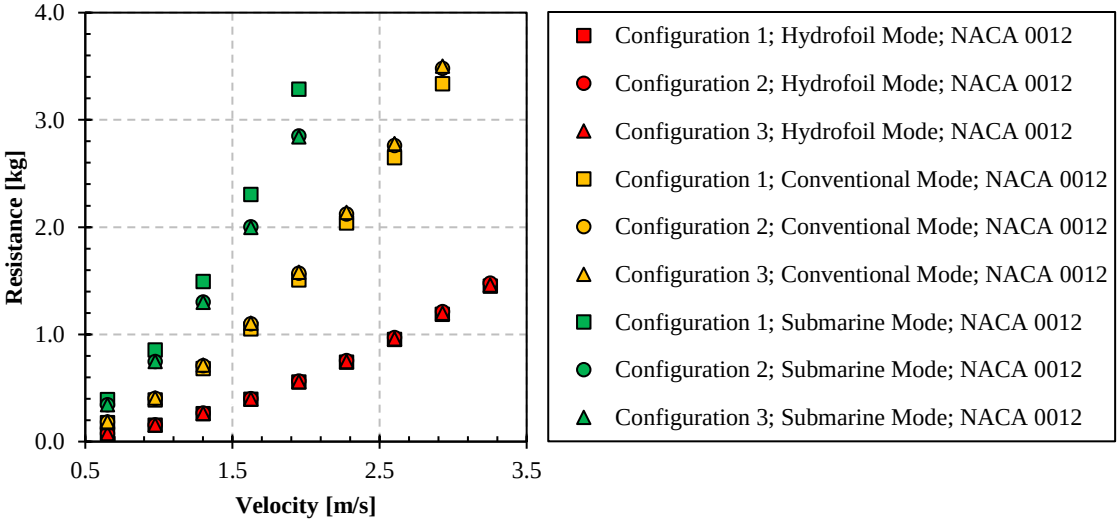

Figure 10 Ship resistance for NACA 0012

The simulation results for the NACA 0012 configuration in hydrofoil mode was observed to show an average increase of 47% compared to configuration 1 as indicated in Figure 10. The alteration of the NACA profile was discovered to have led to the reduction of the resistance. This was confirmed by the resistance value of 1.4 kg recorded for the Configuration 3 (hydrofoil mode and NACA 0012) and 2 kg for Configuration 3 (hydrofoil mode and NACA 0016). The difference in the reduction of the resistance was likely due to the variance in NACA thickness.

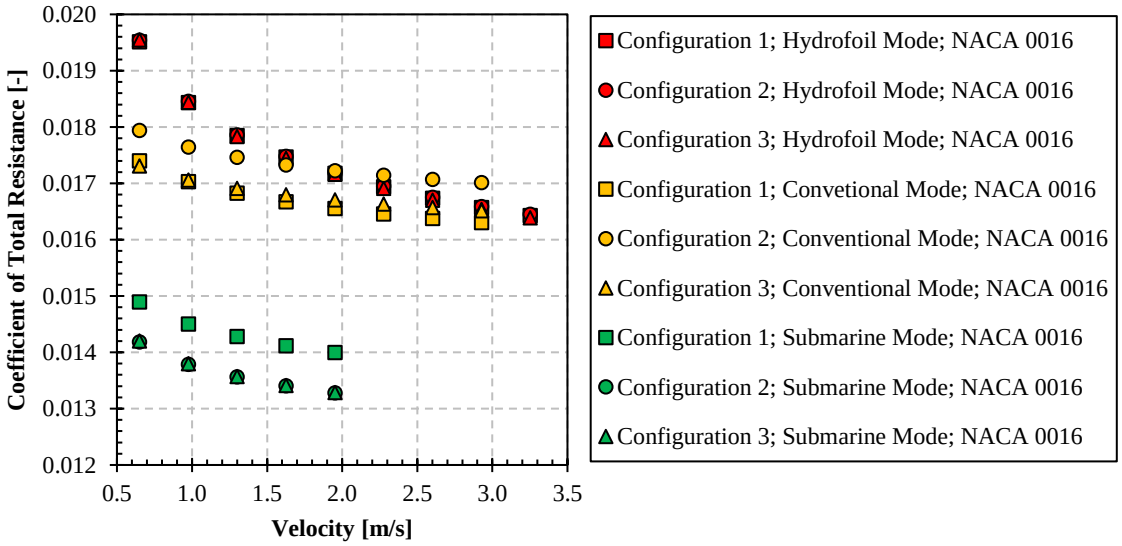

Figure 11 Coefficient of Total Resistance (C_T) for NACA 0016

The simulation conducted in relation to the influence of velocity and configuration on the total resistance coefficient are presented in Figure 11. The results generally showed that the total resistance coefficient reduced as the velocity increased. To determine the effectiveness of the configurations, average percentage reductions in total resistance coefficients were calculated based on the largest and smallest data values for each configuration. Furthermore, the hybrid mini-submarine with NACA 0016 hydrofoil shape configuration exhibited the lowest average total resistance coefficient in position Configuration 3 as indicated by 2.16% recorded for the hydrofoil, 0.66% for the conventional, and 1.64% for the submarine mode. The trend confirmed that the total resistance coefficient was dependent on the velocity of the ship. This was mainly due to the fact that a fast-moving ship normally encounters greater resistance. However, the relationship between the total resistance coefficient and velocity was observed not to be always linear and varied depending on the design and characteristics of the ship. This was confirmed by the non-linear or exponential pattern observed for the total resistance coefficient of the hydrofoil mode while the conventional and submarine modes tended to have a linear pattern. The phenomenon further supported the notion that ships with hydrofoil mode experienced lower resistance. These results were discovered to be similar to those reported in several previous studies. For example, [16] estimated a 22% to 36% increase in the total resistance coefficient because of the factors such as surface roughness, changes in velocity, and the ratio of draft depth.

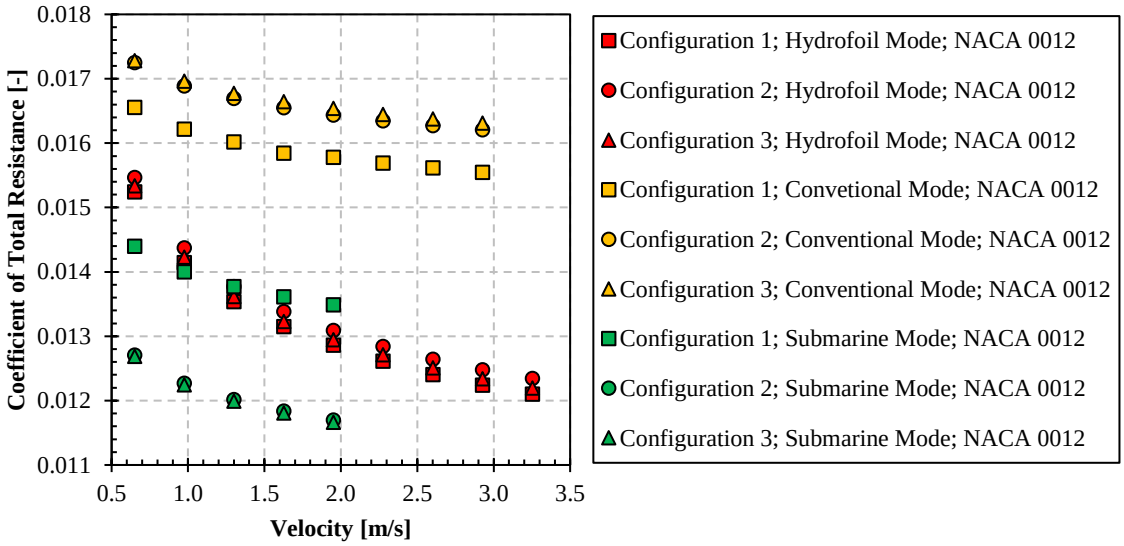

Figure 12 Coefficient of Total Resistance (C_T) for NACA 0012

The hybrid mini-submarine with NACA 0012 hydrofoil configuration was found to have the lowest total resistance coefficient in position Configuration 1 as indicated by the 2.82% recorded for the hydrofoil, 0.89% for the conventional, and 1.62% for the submarine mode in Figure 12. The total resistance coefficient was also typically lower due to the relatively small flow velocity around the hull of the ship but tended to increase as the flow velocity became greater, leading to increased turbulence and pressure.

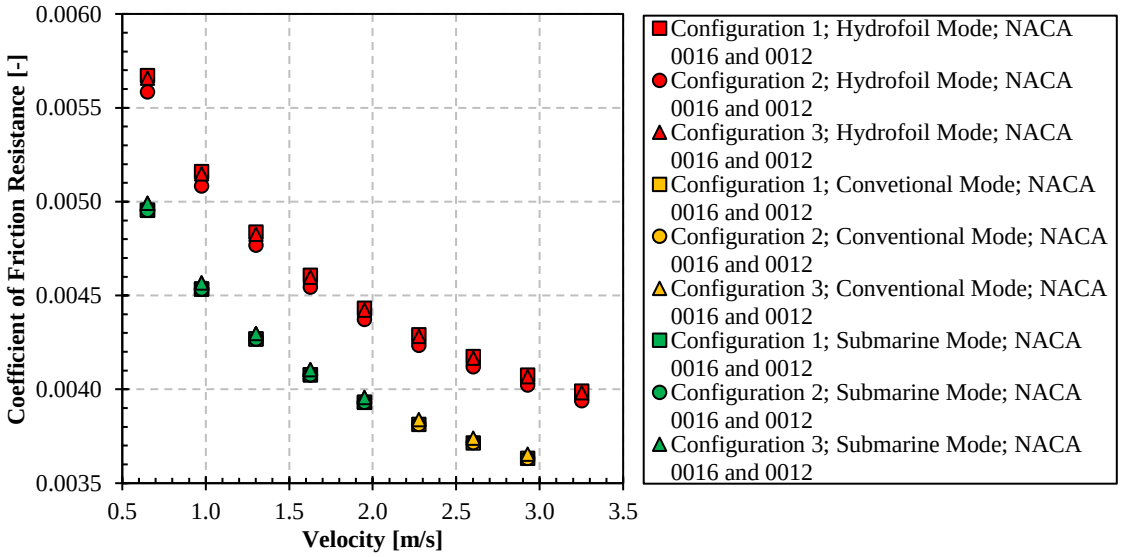

Figure 13 Coefficient of Friction Resistance (C_F) for the Hybrid Mini-Submarine

The results of the influence of velocity and configuration on the friction coefficient were presented in Figure 13 and the friction coefficient was observed to reduce as the velocity increased. The hybrid mini-submarines with NACA 0016 and 0012 configurations were also indicated to exhibit the lowest average friction coefficient in position Configuration 2. The friction coefficient generally remained constant as the velocity increased but this can change due to some effects. For example, the value can reduce when the static friction force is greater than the kinetic friction force, thereby making

the object to move. Once the object reaches and maintains a constant velocity, the friction coefficient can remain constant. The results further showed that the friction coefficient of the ships in hydrofoil, conventional, and submarine modes followed an exponential pattern. This was confirmed by [17] that an increase in the friction coefficient led to a reduction in ship velocity and an increase in fuel consumption.

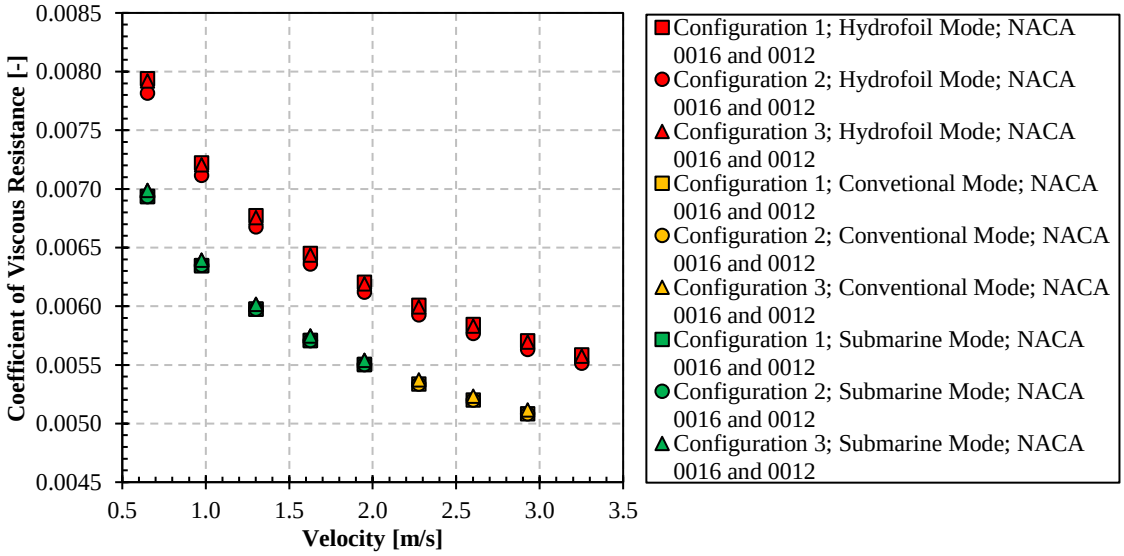

Figure 14 Coefficient of Viscous Resistance (C_V) for the Hybrid Mini-Submarine

The influence of speed and configuration on the viscosity resistance coefficient presented in Figure 14 showed that the viscosity resistance coefficient generally reduced as the speed increased. Moreover, viscosity resistance coefficient was observed to have a greater influence compared to the friction resistance coefficient. The viscosity resistance coefficient for NACA 0016 and 0012 configurations were also discovered to exhibit the highest values among all the hydrofoil modes. The values were observed not reduce generally as the speed increased but they were locally altered by the effect of the speed on the fluid flow properties. The results also showed that the flow tended to be laminar at low Reynolds numbers, resulting in higher viscosity resistance coefficients but became turbulent at high numbers, leading to lower coefficients. However, these changes depended on the fluid properties and the shape of the flow. This indicated the increase or decrease in the viscosity resistance coefficient value as the speed increased depended on the existing flow conditions. The results further confirmed that the friction resistance coefficient of ships in hydrofoil, conventional, and submarine modes followed an exponential pattern.

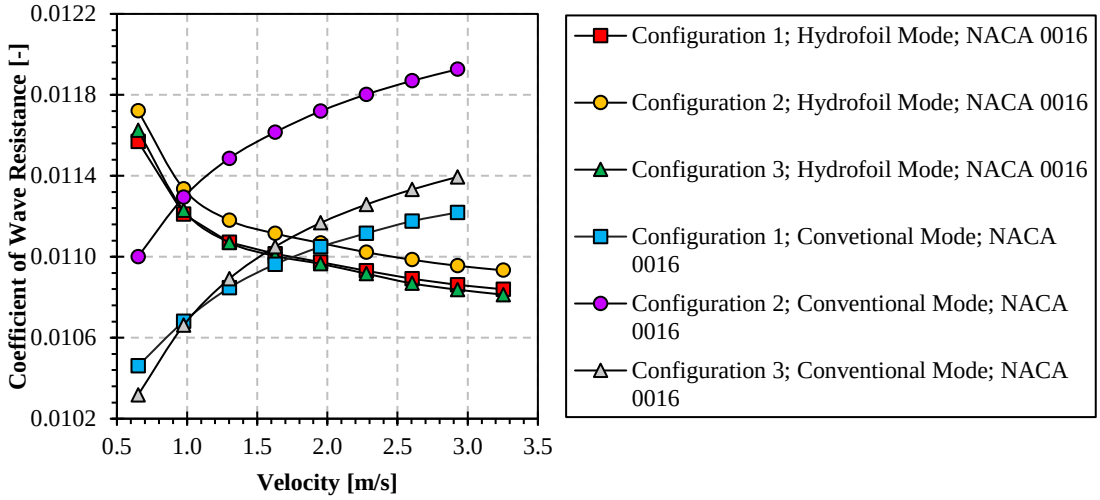

Figure 15 Coefficient of Wave Resistance (C_W) for NACA 0016

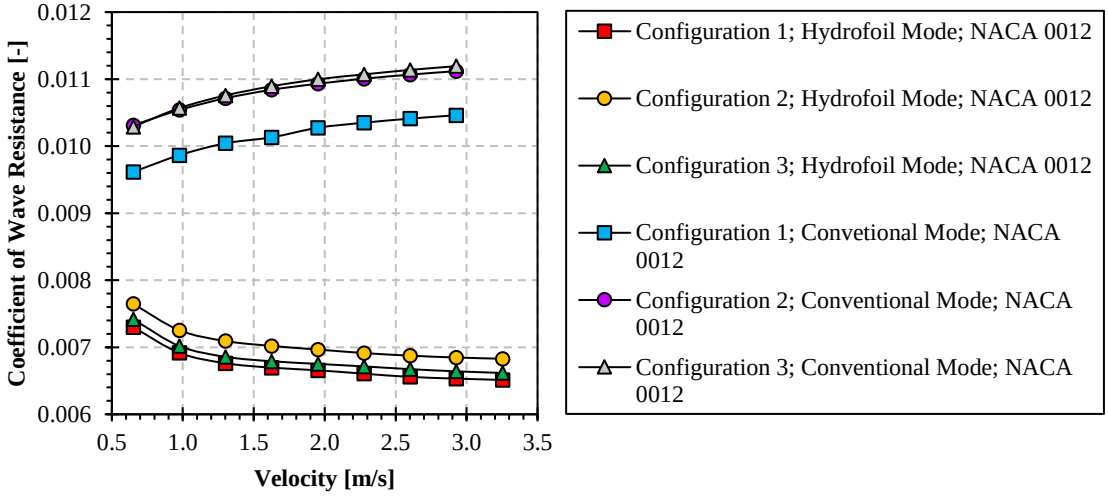

Figure 16 Coefficient of Water resistance (C_W) for NACA 0012

The wave resistance coefficient values were observed to be increasing as the ship speed increased only in the conventional mode as indicated in Figures 15 and 16. This was because the Wetted Surface Area (WSA) of the ship, which came in contact with the water, was larger in the conventional mode compared to the hydrofoil mode, resulting in lower wave resistance coefficient values. Moreover, the NACA 0016 configuration had the highest increase of 1.43% for the wave resistance coefficient in the conventional mode at position 3 and the highest decrease of 0.9% in the hydrofoil mode at position 3. A similar trend was observed in the NACA 0012 configuration with the highest increase, 1.21%, recorded for the wave resistance coefficient in conventional mode at position 1 and the highest decrease, 1.40%, in the hydrofoil mode at position 1.

The waves generated were observed to generally become bigger as the speed of the ship increased. This was associated with the maintenance of constant waterline by fast-moving ships, making it more challenging to move through the water quickly. Therefore, the wave resistance coefficient needed to be reduced in order to enhance the operational efficiency and reduce the fuel costs. resistance coefficient needed to be accurately calculated to determine the energy required for a ship to move forward and also considered highly valuable in designing more efficient ship propulsion systems.

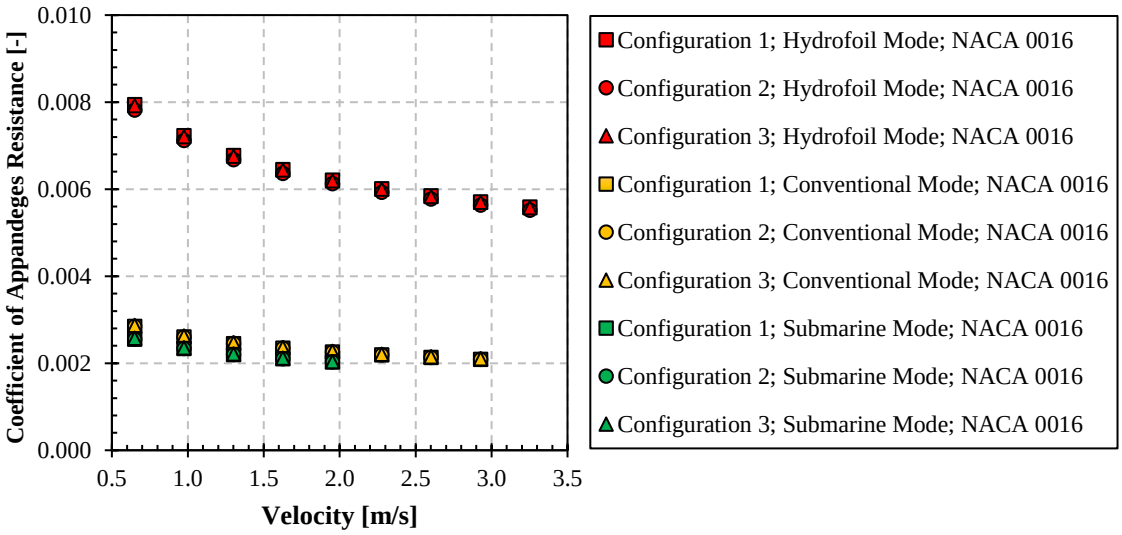

Figure 17 Coefficient of Appendages Resistance for NACA 0016

The influence of speed and configuration on the resistance coefficient of appendages was presented in Figure 17 and it was discovered that the hybrid mini-submarine with NACA 0016 exhibited the highest average reduction in resistance across all modes. The term "appendages" was used in this study to indicate additional structures such as hydrofoils contributing to the increase in hydrodynamic resistance or drag force. The application of this factor was considered to have a significant impact on the hydrodynamic characteristics of a ship, particularly when in close proximity to the fluid surface [18]. This was due to the fact that the appropriate inclusion of appendages can enhance ship stability, reduce drag forces, and improve overall performance.

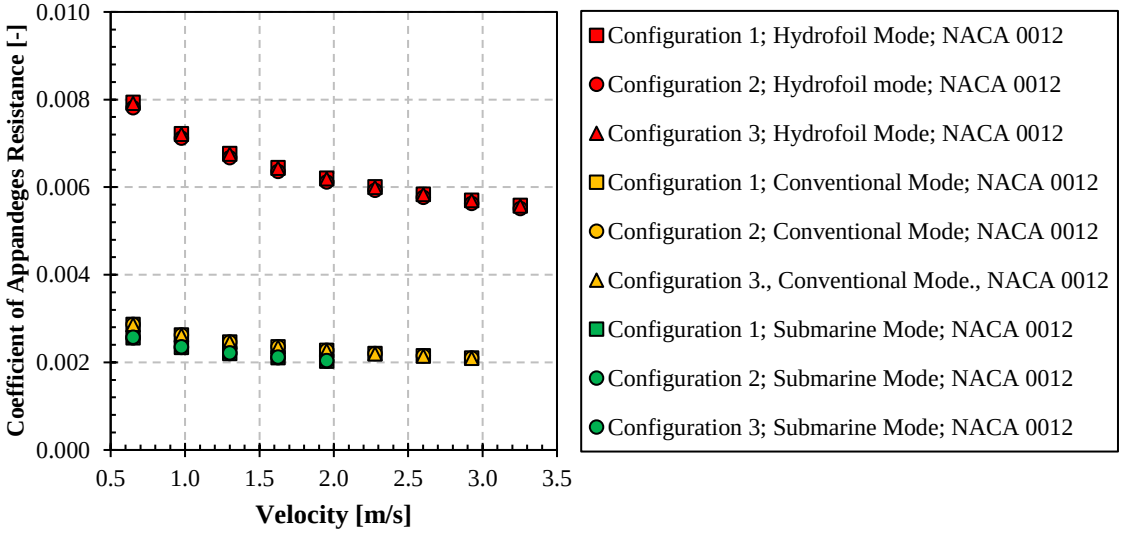

Figure 18 Graph of appendages resistance coefficient calculation for NACA 0012

The resistance coefficient of NACA 0012 appendages was presented in Figure 18 and it was generally observed that the trend was similar to NACA 0016 appendages. This confirmed that the shape and configuration of NACA did not affect the drag of appendages. Meanwhile, Shariati and Mousavizadegan (2017) argued that the optimal type and size of appendages varied depending on the speed of the ship, angle of attack, and draft [18].

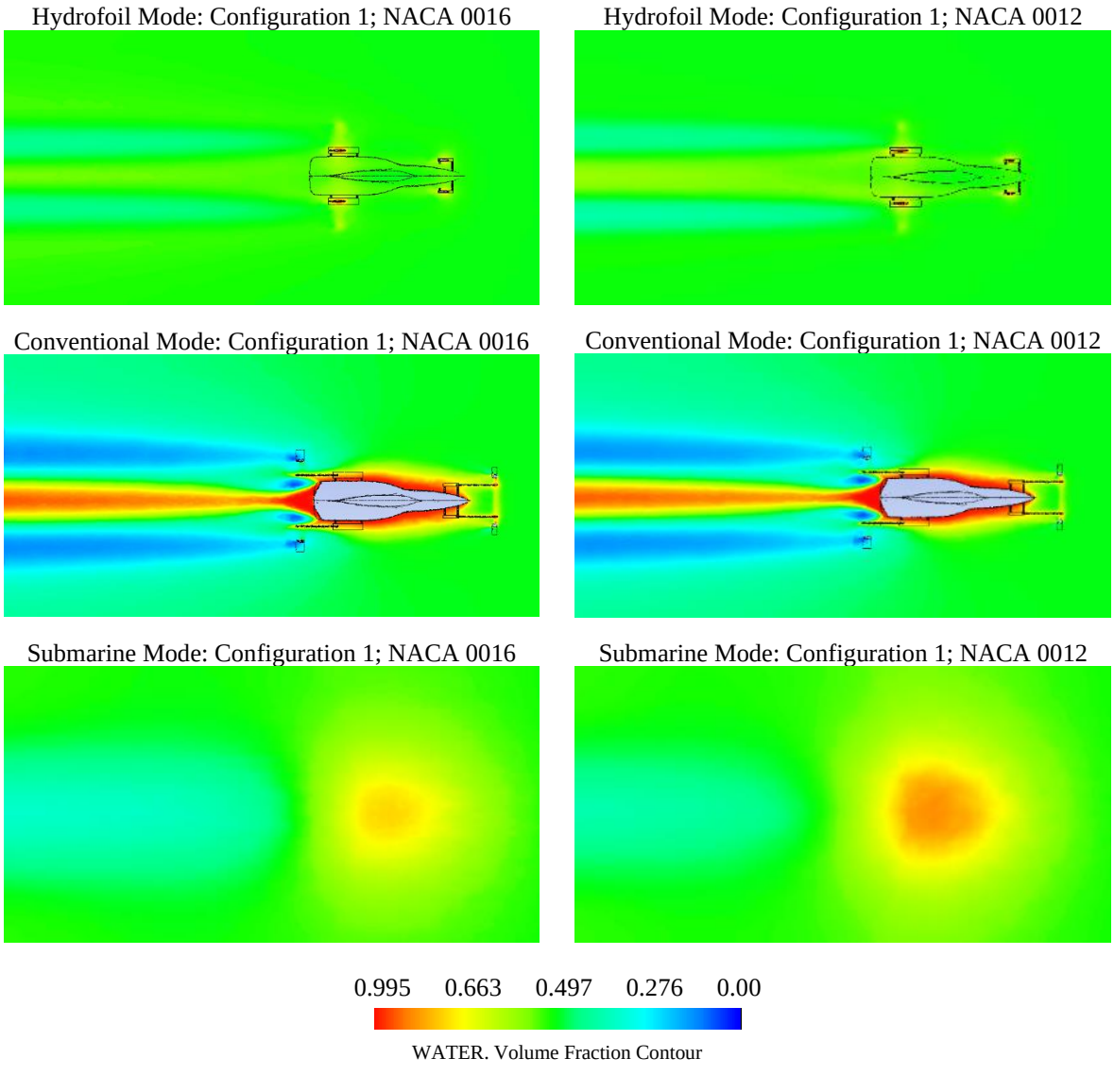

Figure 19 Ship wave contour for all modes

The coefficient of appendage for the NACA 0012 is presented in Figure 19 and the results showed that the values closely resembled those recorded for NACA 0016. This also confirmed that the shape and configuration of the NACA profiles did not significantly affect the appendage drag. In contrast, Shariati and Mousavizadegan argued that the optimal type and size of appendages varied depending on the speed of the ship, angle of attack, and draft [18]. A hybrid mini-submarine model was simulated at a speed of 3.25 m/s for the hydrofoil mode (configuration 1; NACA 0016) in Figure 19 and the results showed that the hydrofoil significantly reduced resistance, as indicated by the absence of large waves generated by the submarine. Moreover, the wave contour of the NACA 0016 showed similar characteristics across different positions, with minor variations in the wave elevation. Meanwhile, the wave contour of the hydrofoil mode (configuration 1; NACA 0012) at a speed of 3.2534 m/s showed the highest elevations around the strut foils, both at the fore and aft. The

hydrofoil in this mode also played a significant role in drag reduction.

The contour of the conventional mode (configuration 1; NACA 0016) was simulated at a speed of 2.928 m/s and the results showed that the wave contour of the NACA 0016 exhibited consistent characteristics at different positions. However, slight variations were recorded in the elevation primarily due to diffracted waves. A similar trend was reported for the conventional mode (configuration 1; NACA 0012) as indicated by the existence of slight but not significant variations in wave elevation at the same speed.

The wave contour of the submarine mode (Configuration 1; NACA 0016) was also observed to demonstrate similar characteristics across different positions at a speed of 1.952 m/s, as evidenced by the comparable total resistance values. Meanwhile, the contour of the submarine mode (configuration 1; NACA 0012) did not show the shape of the submarine at the same speed due to its submerged position. It was discovered that this mode exhibited the highest resistance among all the modes due to the fully submerged body of the submarine. According to Song *et al*., the vortex volume was evenly distributed along the contour and the amplitude of the lift coefficient remained constant in submarine simulations [19]. The pressure values and vortex intensities in the rear part of the submarine were also closely related to speed while their distribution was relatively associated with velocity [20]. Moreover, the unstable characteristics of the submarine model without a protective layer tended to be generally more pronounced.

4.0 CONCLUSION

In conclusion, the implementation of hydrofoil technology on ships reduced resistance and enhanced ship efficiency. This was confirmed through the simulation of a hybrid mini submarine configured with different NACA hydrofoil positions and shapes using Ansys CFX software. The hydrofoil mode was observed to have generated less resistance compared to conventional and submarine modes. This means the utilization of hydrofoils could decrease drag, thereby leading to lower operational costs and reduced environmental impact of maritime transportation.

The positions and shapes linked to each NACA hydrofoil configuration were observed to have a significant impact on the hybrid mini submarine. However, Configuration 3 in NACA 0016 and 0012 was observed to have the lowest resistance compared to 1 and 2. All the position configurations tested using NACA 0012 also showed better resistance characteristics compared to those in NACA 0016 due to the more streamlined shape of NACA 0012 as well as its smaller wetted area.

Configuration 3 with the closest distance between hydrofoils was observed to have the best performance among all the modes tested using both NACA 0016 and 0012 hydrofoils. Moreover, Configuration 3 in NACA 0012 hydrofoil provided the highest reduction in resistance with 12.52%.

The addition of appendages was generally observed to have a significant influence on the hydrodynamic characteristics of ships, particularly when they were close to the surface. This means the proper implementation of appendages could enhance ship stability, reduce drag forces, and improve overall performance. The drag coefficients of NACA 0012 and NACA 0016 appendages were found to be similar, but the optimal types and sizes were different based on the speed of the ship, angle of attack, and depth. Therefore, appendages should be carefully designed and implemented in ships to maximize their positive effects on the hydrodynamic characteristics.

Conflicts of Interest

The author(s) declare(s) that there is no conflict of interest regarding the publication of this paper.

Acknowledgement

This research was supported by the Universitas Pembangunan Nasional Veteran Jakarta through the Penelitian Dosen S3 (NON SERDOS) PN230386

References

[1] Burke, L., Reytar, K., Spalding, M., and Perry, A. 2012. Reefs at risk revisited in the Coral Triangle. World Resources Institute.

[2] Dirhamsyah, D., Umam, S., and Arifin, Z. 2022. Maritime Law Enforcement: Indonesia's Experience against Illegal Fishing. *Ocean Coast Manag*. 229: 106304.

[3] Sakti, A. S. and Utama, I. K. A. P. 2012. Analisis CFD dan Eksperimen Hambatan Lambung Katamaran Asimetris Flat Side Outside dengan Variasi Jarak Demihull. *Jurnal Teknik ITS*. 1: 78-83.

[4] Kundu, P., Sarkar, A., and Nagarajan, V. 2019. Improvement of Performance of S1210 Hydrofoil with Vortex Generators and Modified Trailing Edge. *Renew Energy*. 142: 643-657.

[5] Kusuma, M. R. D. A., Chrismianto, D., and Jokosiworo, S. 2017. Pengaruh Posisi Foil Terhadap Gaya Angkat dan Hambatan Kapal Katamaran. *Kapal: Jurnal Ilmu Pengetahuan dan Teknologi Kelautan*. 14: 58-64.

[6] Budiyanto, M. A., Murdianto, M. A., and Syahrudin, M. F. 2020. Study on the Resistance Reduction on High-speed Vessel by Application of Stern Foil using CFD Simulation. *CFD Letters*. 12: 35-42.

[7] Kazemi Moghadam, H., Shafaghat, R., and Hajiabadi, A. 2019. Foil Application to Reduce Resistance of Catamaran under High Speeds and Different Operating Conditions. *International Journal of Engineering*. 32: 106-111.
[8] Liu, S., He, G., Wang, Z., Luan, Z., Zhang, Z., Wang, W., *et al*. 2020. Resistance and Flow Field of a Submarine in a Density Stratified Fluid. *Ocean Engineering*. 217: 107934.
[9] Sarraf, S., Abbaspour, M., Dolatshahi, K. M., Sarraf, S., and Sani, M. 2022. Experimental and Numerical Investigation of Squat Submarines Hydrodynamic Performances. *Ocean Engineering*. 266: 112849.
[10] Wardhana, W., Wardhana, E. M., Soetardjo, M., and Nichita, O. F. 2021. Naval Architectural Aspects in the Design of a Hybrid Hydrofoil-submarine Craft. *IOP Conference Series: Materials Science and Engineering*. IOP Publishing. 012010.
[11] Wardhana, W., Soetardjo, M., Wardhana, E., and Sujantoko, S. 2020. Analyze of Crocodile Ship Prototype Hull Resistance in Hydrofoil Mode. EasyChair.
[12] Birk, L. 2019. *Fundamentals of Ship Hydrodynamics: Fluid Mechanics, Ship Resistance and Propulsion.* John Wiley & Sons.
[13] Moonesun, M., Ghasemzadeh, F., Korol, Y., Valeri, M., Yastreba, A., and Ursalov, A. 2017. Effective Depth of Regular Wave on Submerged Submarines and AUVs. *International Robotics & Automation Journal*. 2: 208-216.
[14] Huang, P., Bardina, J., and Coakley, T. 1997. Turbulence Modeling Validation, Testing, and Development. *NASA Tech Memo*. 110446: 10-2514.
[15] Murai, Y., Sakamaki, H., Kumagai, I., Park, H.J., and Tasaka, Y. 2020. Mechanism and Performance of a Hydrofoil Bubble Generator Utilized for Bubbly Drag Reduction Ships. *Ocean Engineering*. 216: 108085.
[16] Song, Y., Ming, P., and Yu, G. 2023. Research on Unsteady Characteristics of Different Appendaged Submarines Flows Based on Dynamic Mode Decomposition. *Ocean Engineering*. 276: 114189.
[17] Hakim, M. L., Suastika, K., and Utama, I. 2023. A Practical Empirical Formula for the Calculation of Ship Added Friction-Resistance Due to (Bio) Fouling. *Ocean Engineering* 271(40): 113744.
[18] Shariati, S. K. and Mousavizadegan, S. H. 2017. The Effect of Appendages on the Hydrodynamic Characteristics of an Underwater Vehicle Near the Free Surface. *Applied Ocean Research*. 67: 31-43.
[19] Song, S., Terziev, M., Tezdogan, T., Demirel, Y. K., Muscat-Fenech, C. D. M., and Incecik, A. 2023. Investigating Roughness Effects on Ship Resistance in Shallow Waters. *Ocean Engineering*. 270: 113643.
[20] Chillcce, G., & el Moctar, O. 2022. Viscous Effects on Squat. *Applied Ocean Research*. 125: 103252.